AMERICAN SOCIETY FOR MICROBIOLOGY | Applied and Environmental Microbiology®

FOOD MICROBIOLOGY

Stress Resistance and Pathogenicity of Nonthermal-Plasma-Induced Viable-but-Nonculturable *Staphylococcus aureus* through Energy Suppression, Oxidative Stress Defense, and Immune-Escape Mechanisms

Xinyu Liao,[a] Weicheng Hu,[b] Donghong Liu,[a] Tian Ding[a]

[a]College of Biosystems Engineering and Food Science, Zhejiang Key Laboratory for Agro-Food Processing, Zhejiang University, Hangzhou, China

[b]Jiangsu Collaborative Innovation Center of Regional Modern Agriculture & Environmental Protection/Jiangsu Key Laboratory for Eco-Agricultural Biotechnology around Hongze Lake, School of Life Sciences, Huaiyin Normal University, Huaian, China

ABSTRACT The occurrence of viable-but-nonculturable (VBNC) bacteria poses a potential risk to food safety due to failure in conventional colony detection. In this study, induction of VBNC *Staphylococcus aureus* was conducted by exposure to an atmospheric-pressure air dielectric barrier discharge-nonthermal-plasma (DBD-NTP) treatment with an applied energy of 8.1 kJ. The stress resistance profiles and pathogenicity of VBNC *S. aureus* were further evaluated. We found that VBNC *S. aureus* showed levels of tolerance of heat, acid, and osmosis challenges comparable to those shown by culturable *S. aureus*, while VBNC *S. aureus* exhibited enhanced resistance to oxidative and antibiotic stress, relating to the mechanisms of cellular energy depletion, antioxidant response initiation, and multidrug efflux pump upregulation. Regarding pathogenicity, NTP-induced VBNC *S. aureus* retained the capacity to infect the HeLa host cells. Compared with the culturable counterparts, VBNC *S. aureus* caused reduced immune responses (Toll-like receptor [TLR], nucleotide-binding oligomerization domain [NOD]) in HeLa cells, which was attributed to suppression of biosynthesis of the recognized surface ligands (e.g., peptidoglycan). Additionally, the proteomic analysis revealed that upregulation of several virulence factors (ClfB, SdrD, SCIN, SasH, etc.) could ensure that VBNC *S. aureus* would adhere to and internalize into host cells and avoid the host attack. The camouflaged mechanisms described above led to VBNC *S. aureus* causing less damage to the host cells, and their activity might result in longer intracellular persistence, posing potential risks during NTP processing.

IMPORTANCE The consumer demand for freshness and nutrition has accelerated the development of mild decontamination technologies. The incomplete killing of nonthermal (NT) treatments might induce pathogens to enter into a viable-but-nonculturable (VBNC) status as a survival strategy. The use of nonthermal plasma (NTP) as a novel food decontamination technology received increased attention in food industry during recent decades. Our previous work confirmed that the foodborne pathogen *S. aureus* was induced into VBNC status in response to NTP exposure. This work further revealed the development of stress resistance and virulence retention of NTP-induced VBNC *S. aureus* through the mechanisms of energy suppression, oxidative stress defense, and immune escape. The data provide fundamental knowledge of the potential risks posed by NTP-induced VBNC *S. aureus*, which require further parameter optimization of the NTP process or combination with other techniques to avoid the occurrence of VBNC bacteria.

KEYWORDS viable but nonculturable, stress resistance, oxidative stress defense, pathogenicity, immune escape, virulence factors

Citation Liao X, Hu W, Liu D, Ding T. 2021. Stress resistance and pathogenicity of nonthermal-plasma-induced viable-but-nonculturable *Staphylococcus aureus* through energy suppression, oxidative stress defense, and immune-escape mechanisms. Appl Environ Microbiol 87:e02380-20. https://doi.org/10.1128/AEM.02380-20.

Editor Johanna Björkroth, University of Helsinki

Address correspondence to Tian Ding, tding@zju.edu.cn.

Received 28 September 2020
Accepted 14 October 2020
Accepted manuscript posted online 23 October 2020
Published 4 January 2021

The viable-but-nonculturable (VBNC) state is known as a common survival strategy that bacteria employ against external stresses (e.g., starvation, cold) (1). VBNC bacteria are characterized as failing to form colonies on solid medium but still possessing metabolic activities. VBNC status renders to bacteria the capacity to escape from detection by conventional plate count methods (2). Apart from the challenge of nonculturability, VBNC bacteria have been shown to retain or even increase their virulence in previous studies. Nowakowska and Oliver (3) found that VBNC *Vibrio vulnificus* showed enhanced tolerance of a range of stressors (e.g., heat, oxidation, osmosis). Apart from resistance development, pathogenesis was also reported to be retained in VBNC pathogens. The Shiga-like toxin genes (stx_1, stx_2) could be still detected while *Escherichia coli* O157:H7 stayed in a VBNC status (4). In a study previously reported by Highmore et al. (5), it was found that chlorine-induced VBNC *Listeria monocytogenes* and *Salmonella enterica* could infect *Caenorhabditis elegans* in a manner similar to that seen with their culturable counterparts. However, some conflicting data were found in other studies regarding the virulence of VBNC bacteria. Zhao et al. (6) demonstrated that *E. coli* O157:H7 had lost the capacity to infect HeLa cells after entering the VBNC status.

In recent years, several physical and chemical treatments along food processing have been reported to induce bacteria into a VBNC state. For instance, Zhao et al. (6) confirmed that high-pressure CO_2 treatment forced *E. coli* O157:H7 into the VBNC state. Liao et al. (7) observed the induction of approximately 2 to 3 logs VBNC *Salmonella* Typhimurium by thermosonication hurdle processing. Citric acid, a common food preservative, was reported to have mediated a transition of *Staphylococcus aureus* into the VBNC state after an 18-day exposure (8). Additionally, chlorine washing has been demonstrated to induce both *Listeria monocytogenes* and *Salmonella enterica* serovar to transition into the VBNC state (5). Therefore, the potential risk represented by the presence of VBNC bacteria should be carefully taken into consideration during the development of novel food processing technologies in order to ensure food safety.

Nonthermal-plasma (NTP) technology has gained increasingly global interest in the last 2 decades (9, 10). As an alternative decontamination technology, NTP has been applied to a wide range of food, including beverages, meat and poultry, vegetables, and fruits (11, 12). The advantages of low working temperature ($<$60°C), high antimicrobial efficacy, absence of water and solvent, and reduced compromise of food quality make the use of NTP a sustainable and environmentally friendly method to ensure food safety (13, 14). However, the effect of NTP on microbial behavior is still not fully understood. Some studies have observed the occurrence of VBNC bacteria during NTP treatments (15, 16). The molecular mechanisms used for NTP induction of VBNC *S. aureus* were also explored in our previous study (17). However, the changes related to the resistance and pathogenicity of NTP-induced VBNC pathogens are still unclear.

In this study, a dielectric barrier discharge (DBD) atmospheric NTP system, operating with a frequency of 10 kHz and a power level of 44.95 W, was used to treat *S. aureus* (17). The upper electrode in DBD-NTP system is covered by a quartz dielectric barrier with a diameter of 90 mm (Fig. 1A), which introduces a large capacitance between two electrodes. When an oscillating current is applied, the charges are accumulated on the dielectric surface and the electric field is reduced. Subsequently, the gas between the electrodes is discharged and produces an effectively uniform volume of nonequilibrium plasma through numerous individual streamer breakdowns. Air, mainly consisting of N_2, O_2, and H_2O, is employed as the working gas, which is discharged in the space (8 mm) between the upper quartz glass (with a diameter of 90 mm) and the bacterial suspension surface. Plasma contains abundant species, including excited atoms/molecules, electrons, positive and negative ions, radical species, and quanta of electromagnetic radiation (UV photons and visible light).

We confirmed previously that the NTP system is able to induce the VBNC *S. aureus* through metabolic suppression and the oxidative stress response (17). Furthermore, we

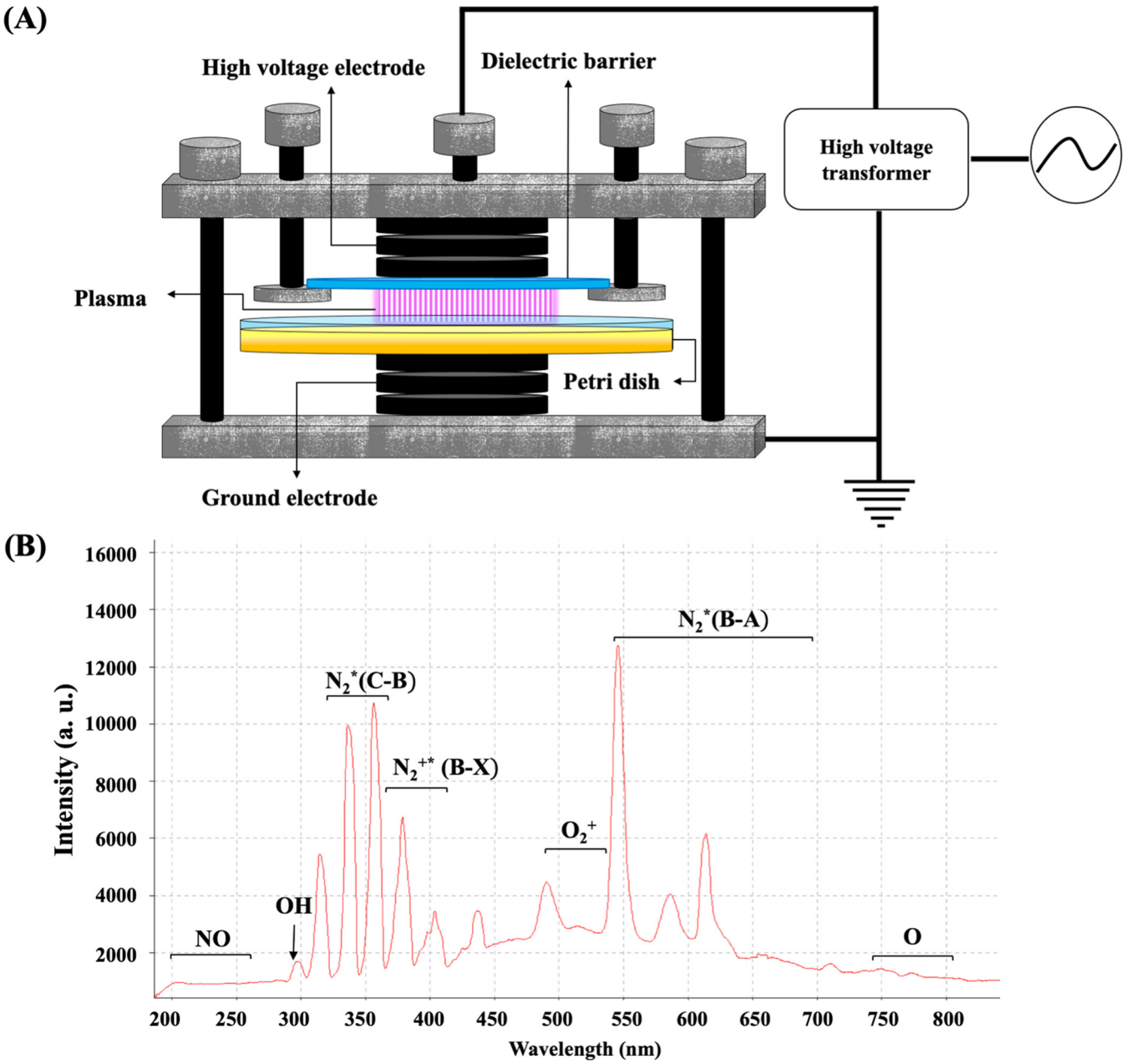

FIG 1 The configuration of the dielectric barrier discharge (DBD) atmospheric air nonthermal-plasma (NTP) system (A) and the associated emission spectrum of the DBD-NTP system at applied energy of 8.1 kJ (B). a.u., arbitrary units.

wondered whether pathogenic bacteria in such a state retain their risks in food safety and human health. Therefore, in this study, we estimated the resistance of NTP-induced VBNC *S. aureus* to common stresses (heat, acid, osmosis, oxidation) and antibiotics (ciprofloxacin, chloramphenicol, trimethoprim, oxacillin). In addition, the capacity of VBNC *S. aureus* to infect HeLa cells was evaluated. With the assistance of a proteomic technique, the changes in virulence factors of VBNC *S. aureus* compared to culturable counterparts were estimated.

RESULTS

Enzymatic activity of VBNC *S. aureus*. As Fig. 2 shows, VBNC *S. aureus* cells retained their activity with respect to alkaline phosphatase (lane 2), esterase C4 (lane 3), esterase lipase C8 (lane 4), acid phosphatase (lane 11), and naphthol-AS-BI-phosphohydrolase (lane 12), while the population of culturable *S. aureus* possessed

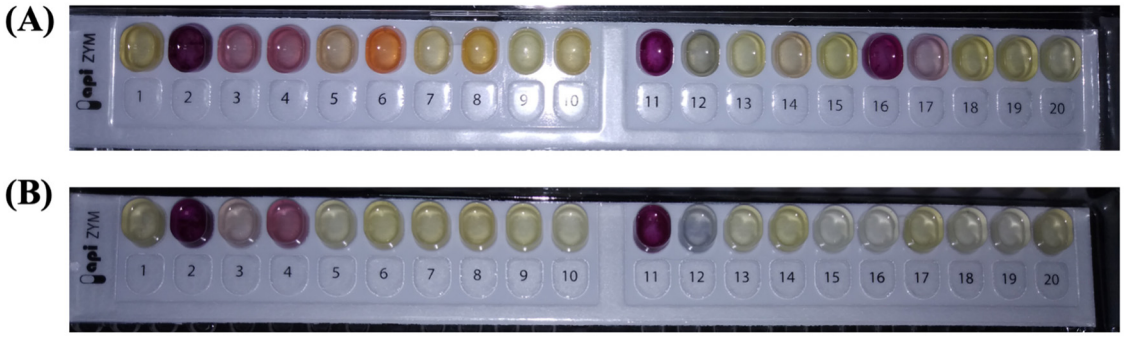

FIG 2 The enzymatic activity of culturable (A) and NTP-induced VBNC (B) *S. aureus*. Lanes 1 to 20 represent the control, alkaline phosphatase, esterase C4, esterase lipase C8, lipase C14, leucine arylamidase, valine arylamidase, cystine arylamidase, trypsin, α-chymotrypsin, acid phosphatase, naphthol-AS-BI-phosphohydrolase, α-galactosidase, β-galactosidase, β-glucuronidase, α-glucosidase, β-gluconidase, N-acetyl-β-glucosaminidase, α-mannosidase, and α-fucosidase, respectively.

another 6 kinds of metabolic enzymes, including lipase C14 (lane 5), leucine arylamidase (lane 6), cystine arylamidase (lane 8), β-galactosidase (lane 14), α-glucosidase (lane 16), and β-glucosidase (lane 17).

Resistance of VBNC *S. aureus* to food-associated stresses. As shown in Fig. 3A to C, the reductions in the levels of VBNC and culturable *S. aureus* caused by heat (63°C), acid (pH 3.0), and osmosis (NaCl 20%) stressors were not statistically significant ($P > 0.05$). Under conditions of exposure to oxidative stress (100 mM H_2O_2) (Fig. 3D), the reductions in the levels of VBNC *S. aureus* cells were significantly ($P < 0.05$) lower than those of the culturable ones, indicating higher tolerance of VBNC *S. aureus* in response to the oxidative stress.

Tolerance of VBNC *S. aureus* toward antibiotics. As exhibited in Fig. 4, the reductions in the levels of VBNC *S. aureus* induced by NTP were significantly lower than those of culturable *S. aureus* after treatment with 10× MIC ciprofloxacin, chloramphenicol, trimethoprim, and oxacillin ($P < 0.05$). Pretreatment with carbonyl cyanide

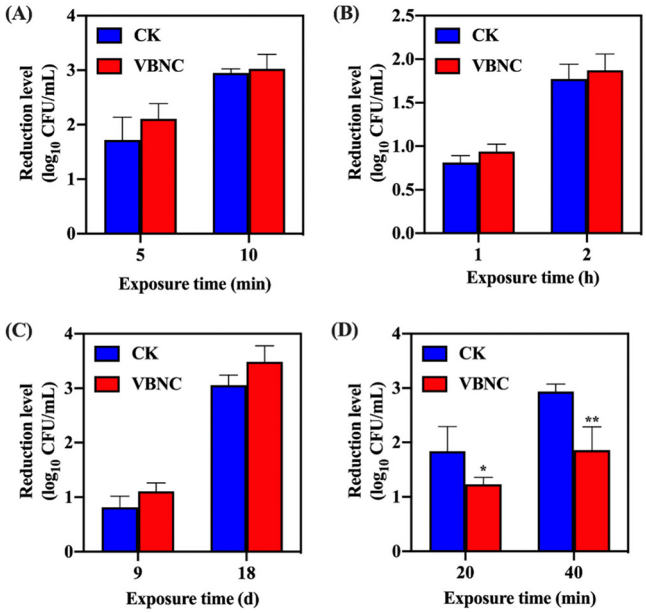

FIG 3 The profile of resistance of viable but nonculturable (VBNC) *S. aureus* to food-associated stresses. (A) Heat stress (63°C). (B) Acid stress (pH 3.0). (C) Osmotic stress (NaCl 20%). (D) Oxidative stress (100 mM H_2O_2). Asterisks indicate statistical significance of results from comparisons between culturable (CK) and VBNC *S. aureus* populations, determined by Student's *t* test (*, $P < 0.05$; **, $P < 0.01$). All experiments were performed in biological triplicate. Standard deviations are represented by the error bars.

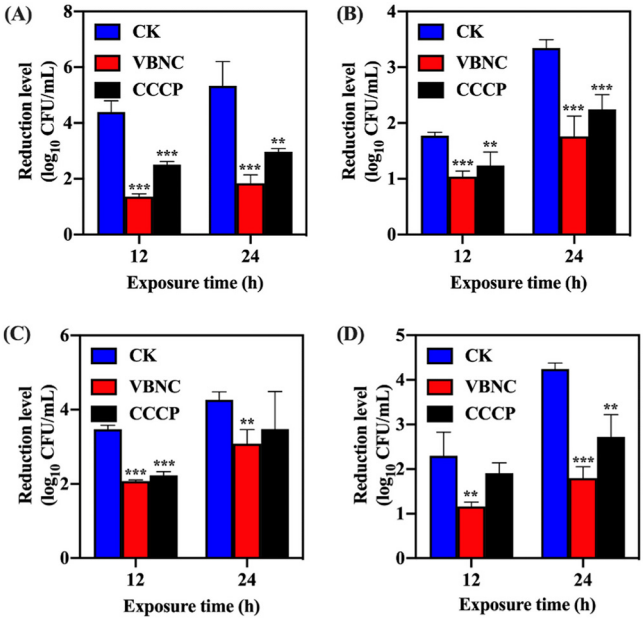

FIG 4 The profile of resistance of viable but nonculturable (VBNC) *S. aureus* to antibiotics: (A) Ciprofloxacin. (B) Chloramphenicol. (C) Trimethoprim. (D) Oxacillin. Asterisks indicate statistical significance of results from comparisons between VBNC *S. aureus* or carbonyl cyanide *m*-chlorophenyl hydrazone-treated *S. aureus* (CCCP) and culturable *S. aureus* (CK), which was determined by Student's *t* test (**, $P < 0.01$; ***, $P < 0.005$). All experiments were performed in biological triplicate. Standard deviations are represented by error bars.

m-chlorophenyl hydrazone (CCCP) also resulted in enhanced resistance of *S. aureus* to the antibiotics stressors compared with their untreated counterparts.

Antioxidative and drug efflux pump expression in VBNC *S. aureus*. As shown in Fig. 5, the expression levels of *dps*, *trxA*, and *katA* related to the antioxidative response in VBNC *S. aureus* were 1.40 ± 0.10, 1.28 ± 0.19, and 1.25 ± 0.12, respectively, which were significantly higher than those of the culturable counterparts ($P < 0.05$). As for the antibiotic efflux pumps, the observed differences between VBNC and culturable *S. aureus* in *mepA*, *norB*, and *ycnB* expression were not statistically significant. However, *lmrS* was an exception and was overexpressed in VBNC *S. aureus*.

Pathogenesis of VBNC *S. aureus* on HeLa cells. As illustrated in Fig. 6, uninfected HeLa cells have intact membrane (red fluorescence) and nucleus (blue fluorescence).

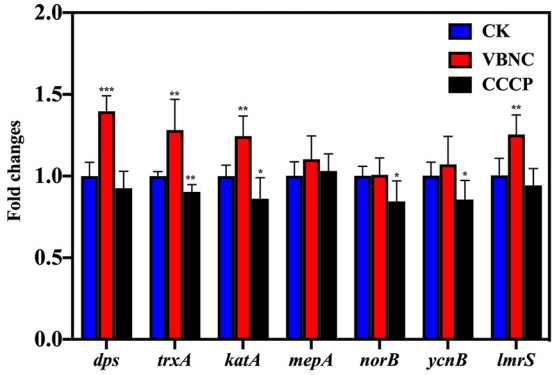

FIG 5 Expression levels of antioxidative genes (*dps*, *trxA*, *katA*) and multidrug efflux pump genes (*mepA*, *norB*, *ycnB*, *lmrS*) in *S. aureus*. Asterisks indicate statistical significance of results from comparisons between viable but nonculturable *S. aureus* (VBNC) or carbonyl cyanide *m*-chlorophenyl hydrazone-treated *S. aureus* (CCCP) and culturable *S. aureus* (CK), which was determined by Student's *t* test (*, $P < 0.05$; **, $P < 0.01$, ***, $P < 0.005$). All experiments were performed in biological triplicate. Standard deviations are represented by error bars.

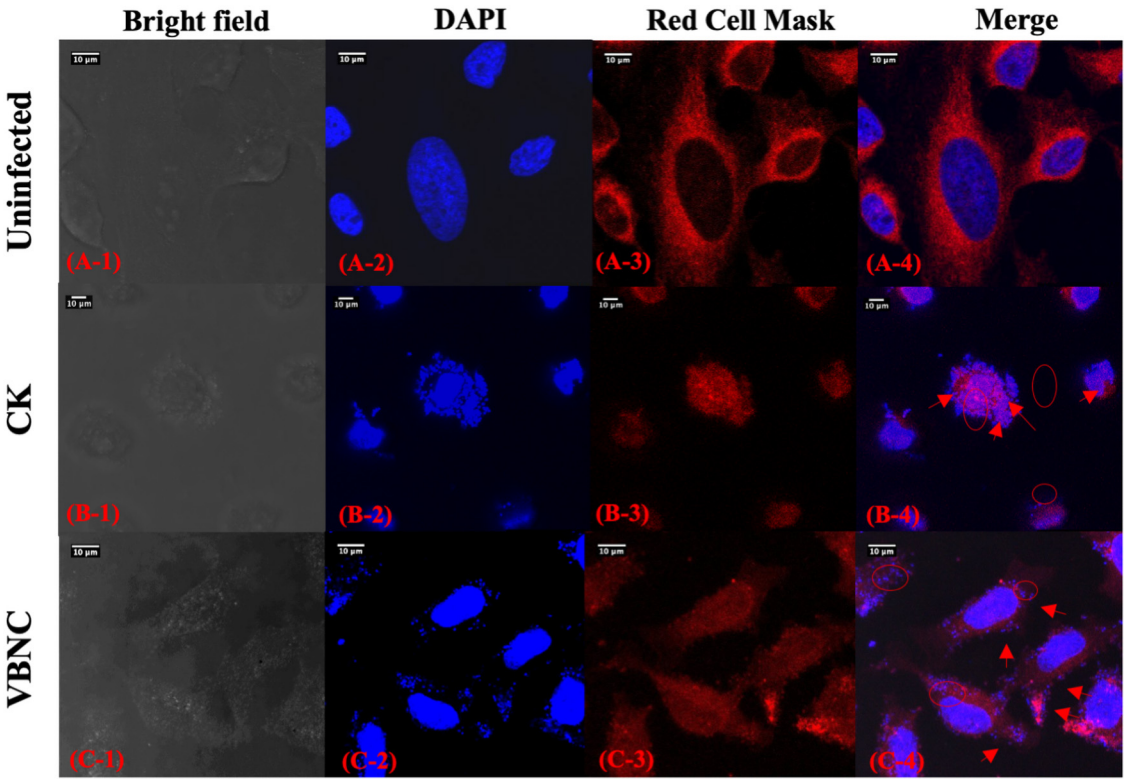

FIG 6 Confocal laser scanning microscopy (CLSM) images of uninfected HeLa cells or HeLa cells infected with culturable (CK) or viable but nonculturable (VBNC) *S. aureus*. Red circles indicate *S. aureus* inside HeLa cells, and red arrows point to *S. aureus* attached to the HeLa cell surface.

Spots of intense blue fluorescence were observed on the surface of and inside the HeLa cells after they were infected by culturable *S. aureus*. In addition, HeLa cells infected with culturable *S. aureus* were seriously deformed, with shrunken nucleus and compromised cell membrane. And the HeLa cells infected with VBNC *S. aureus* cells basically retained a shape similar to that of the uninfected HeLa cells. The number of blue fluorescent spots found on the surface of and inside the VBNC *S. aureus*-infected HeLa cells was lower than the number seen with the culturable *S. aureus*-infected ones.

Immunity response of HeLa cells. The expression levels of immune sensor-related genes in HeLa cells are exhibited in Fig. 7. The *TRL2* and *NOD1* genes in HeLa cells

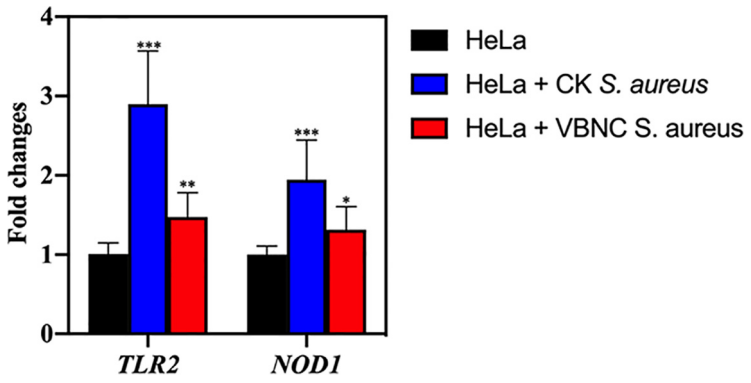

FIG 7 Expression levels of immune genes (encoding TLR2 and NOD1) in HeLa cells. Asterisks indicate statistical significance of results from comparisons between HeLa cells infected with culturable *S. aureus* (CK) or viable but nonculturable *S. aureus* (VBNC) and the uninfected HeLa cells, which was determined by Student's *t* test (*, $P < 0.05$; **, $P < 0.01$; ***, $P < 0.005$). All experiments were performed in biological triplicate. Standard deviations are represented by error bars.

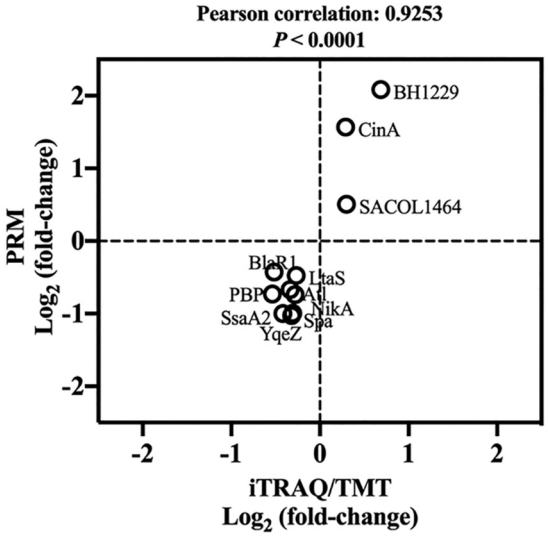

FIG 8 Validation of iTrap/TMT by PRM. The figure shows a plot of protein expression levels determined by the iTrap/TMT and PRM methods for 11 randomly selected proteins. Pearson correlation analysis was conducted. Fold changes in protein levels are expressed as $\log_2$ values.

infected with culturable *S. aureus* were significantly upregulated by 2.90- ± 0.67- and 1.94- ± 0.50-fold, respectively, compared with uninfected HeLa cells. Regarding the HeLa cells infected with VBNC *S. aureus*, the expression level of *TRL2* and *NOD1* were found to be 1.47- ± 0.31- and 1.32- ± 0.29-fold higher than in the uninfected HeLa cells, respectively.

Expression level of virulence-related proteins in VBNC *S. aureus*. As illustrated in Fig. 8, the data determined for 11 randomly selected differentially expressed proteins (DEPs) by the use of iTRAQ/TMT (isobaric tags for relative and absolute quantification/tandem mass tag) and PRM (parallel reaction monitoring) show a Pearson correlation value of 0.9253 ($P < 0.0001$), indicating the reliability of the iTRAQ/TMT method. Based on the proteomics analysis, a total of 41 DEPs functionalized in staphylococcal virulence were found as shown in Table 1. Among these DEPs, the capsular polysaccharide biosynthesis protein (Cap5B), clumping factor (ClfB), adhesin (SdrD), complement inhibitor (SCIN), virulence-associated cell wall-anchored protein (SasH), and Sec-dependent secretory system (SecG, YajC, SecE) were significantly upregulated in VBNC *S. aureus* compared with the culturable counterparts. Other virulence factors were suppressed in NTP-induced VBNC *S. aureus*.

Blood-coagulating activity of VBNC *S. aureus*. As Fig. 9A shows, the negative control (*S. epidermidis*, CMCC 26069) failed to clot the blood after 16 h of incubation. After 4 h of incubation, the blood inoculated with culturable *S. aureus* had clotted as the positive control (*S. aureus* ATCC 29213) did, while VBNC *S. aureus* did not exhibit blood clotting until 16 h of incubation. The culturability of VBNC *S. aureus* was monitored with the plate count method during 16 h of incubation. As Fig. 9B shows, VBNC *S. aureus* became culturable after 4 h of incubation and achieved a culturable level of 7.94 ± 0.5 $\log_{10}$ CFU/ml at the end of 16 h.

Morphological analysis of VBNC *S. aureus*. As shown in Fig. 10A (see also Fig. 11A), culturable *S. aureus* possessed a smooth surface and all of the cells were distributed separately. Regarding VBNC *S. aureus*, a large amount of polymer materials was observed to adhere on the *S. aureus* surface, which resulted in several cells clumping tightly together (Fig. 10B, red arrow). As shown by the atomic force microscopy (AFM) image, VBNC *S. aureus* cells exhibited a quite lumpy surface and the additional materials appeared in the intercellular spaces (Fig. 11B).

DISCUSSION

In our previous study, induction of VBNC *S. aureus* by NTP was confirmed through the suppression of metabolic activity and the induction of oxidative stress response

TABLE 1 Virulence-related differentially expressed proteins in VBNC *S. aureus*[a]

Classification	Protein ID	Description of protein(s)	log_2 FC	*P* value
Capsule	QCY65363.1	Tyrosine-protein kinase/capsular polysaccharide biosynthesis protein Cap5B	0.33	0.0063
Lipoteichoic acid	QCY65886.1	LTA synthase family protein/lipoteichoic acid synthase LtaS	−0.27	0.0223
Peptidoglycan	QCY65288.1	PBP2a family beta-lactam-resistant peptidoglycan transpeptidase	−0.54	0.0078
Lipoprotein	QCY65409.1	Tandem-type lipoprotein	−0.69	0.00062
	QCY65537.1	EfeM/EfeO family lipoprotein	−0.75	0.00083
	QCY65560.1	Tandem-type lipoprotein	−0.45	0.00149
	QCY67403.1	Lipoprotein	−0.32	0.00014
	QCY65601.1	NDxxF motif lipoprotein	−0.32	0.00218
	QCY66887.1	Lipoprotein	−0.85	0.00265
Adherence	QCY66083.1	MHC class II analog protein/MAP domain-containing protein	−1.41	0.0014
	QCY66156.1	Bifunctional autolysin Atl/mannosyl-glycoprotein endo-beta-*N*-acetylglucosamidase	−0.34	0.0151
	QCY66587.1	Elastin-binding protein EbpS	−0.33	7.50E−05
	QCY67246.1	Cell surface protein map-w/MAP domain-containing protein	−0.95	0.00046
	QCY67331.1	MW2217/CHAP domain-containing protein/fibronectin-binding protein	−0.31	0.01575
	QCY67602.1	Probable secretory antigen precursor/CHAP domain-containing protein/ fibronectin-binding protein	−1.25	0.00085
	QCY65963.1	Extracellular matrix protein-binding adhesin Emp/fibronectin-binding protein	−0.61	0.00376
	QCY67533.1	Fibronectin-binding protein FnbA	−0.31	0.01787
	QCY65634.1	Autolysin/adhesin Aaa	−0.31	0.01651
	QCY65730.1	MSCRAMM family adhesin SdrD	0.33	0.00229
	QCY67685.1	MSCRAMM family adhesin clumping factor ClfB	0.32	0.00071

(Continued on next page)

TABLE 1 (Continued)

Classification	Protein ID	Description of protein(s)	log_2 FC	*P* value
Invasion	QCY65327.1	YSIRK signal domain/LPXTG anchor domain surface protein, immunoglobulin G-binding protein A	−0.42	0.01212
	QCY67449.1	Immunoglobulin G-binding protein SBI	−0.56	0.02195
	QCY66897.1	Staphylococcal complement inhibitor SCIN	0.43	0.008048
	QCY65279.1	LPXTG cell wall anchor domain-containing protein SasH	0.31	0.005151
Secretory system	QCY65479.1	Type VII secretion protein EsaA	−0.37	0.000334
	QCY65478.1	WXG100 family type VII secretion effector EsxA	−0.56	3.48E−06
	QCY67622.1	TIGR04197 family type VII secretion effector	−1.25	5.57E−05
	QCY67620.1	DUF4176 domain-containing protein/type VII secretion system extracellular protein C	−0.5	0.004075
Protein translocation	QCY65952.1	Preprotein translocase subunit SecG	0.28	0.005290
	QCY66739.1	Preprotein translocase subunit YajC	0.69	0.000225
	QCY65705.1	Preprotein translocase subunit SecE	2.49	9.81E−05
Toxins	QCY65563.1	Exotoxin 15/superantigen-like protein	−0.48	0.014372
	QCY65566.1	Exotoxin 4	−0.61	8.70E−05
	QCY66274.1	Exotoxin/superantigen-like protein SSL13	−0.47	0.046769
	QCY67583.1	Toxin/exotoxin G SpeG	−0.38	0.002879
	QCY65992.1	Staphylococcal enterotoxin type Q	−0.55	0.018049995
Exoenzymes	QCY66149.1	Cysteine protease staphopain B	−0.58	0.002676
	QCY66150.1	Serine protease	−0.59	0.003407
	QCY67724.1	YSIRK domain-containing triacylglycerol lipase Lip1	−0.26	0.045229
	QCY65517.1	YSIRK domain-containing triacylglycerol lipase Lip2/Geh	−1.05	0.000579
	QCY65427.1	Coagulase	−0.58	0.004444

[a]ECM, extracellular matrix protein; FC, fold change; MHC, major histocompatibility complex; MSCRAMM, microbial surface components recognizing adhesive matrix molecules.

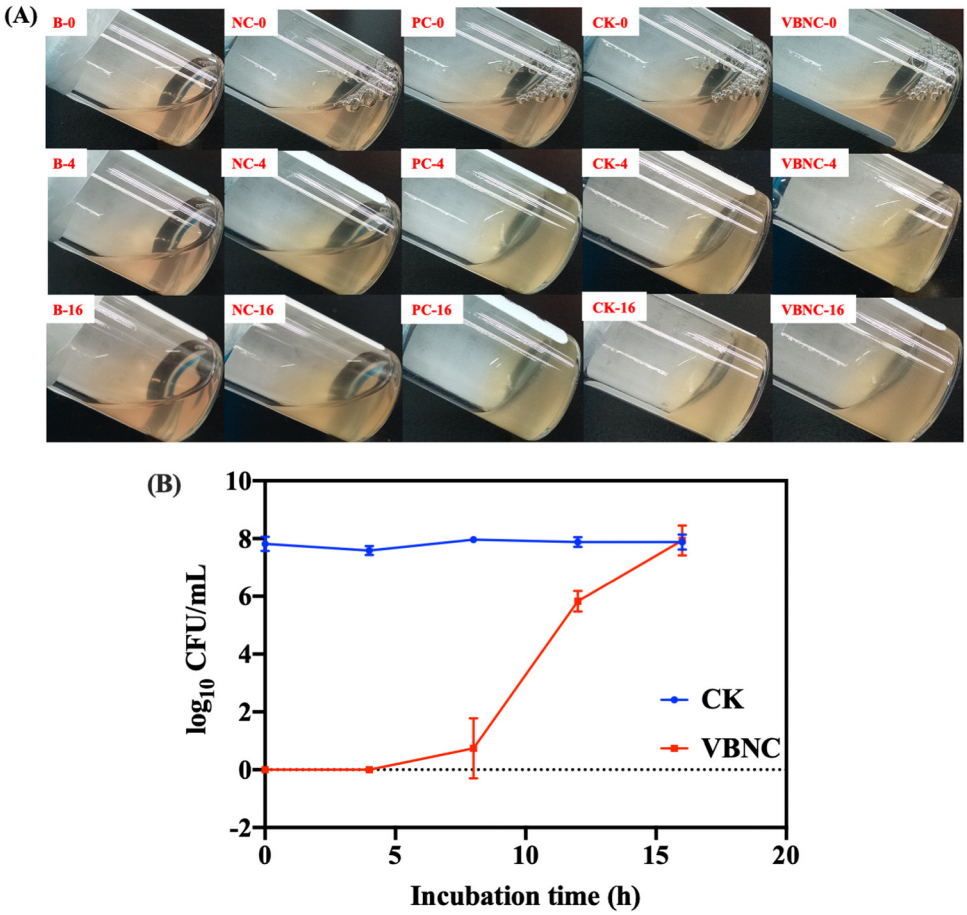

FIG 9 (A) Coagulase test. B-0, B-4, and B-16, blank at 0, 4, and 16 h, respectively; NC-0, NC-4, and NC-16, *S. epidermidis* CMCC 26069 negative control at 0, 4, and 16 h, respectively; PC-0, PC-4, and PC-16, *S. aureus* ATCC 29213 positive control at 0, 4, and 16 h, respectively; VBNC-0, VBNC-4, and VBNC-16, NTP-induced VBNC *S. aureus* at 0, 4, and 16 h, respectively; CK-0, CK-4, and CK-16, culturable *S. aureus* at 0, 4, and 16 h, respectively. (B) Cultivability of VBNC *S. aureus* incubated in rabbit blood.

(17). In this study, we further analyzed the potential risks of NTP-induced *S. aureus* and the related mechanisms. First, the levels of resistance of VBNC and culturable *S. aureus* to the thermal (63°C), acid (pH 3.0), and osmosis (20% NaCl) stressors were not statistically significantly different from those seen with the culturable ones. The result was consistent with the study of Bai et al. (8), who also observed comparable levels of tolerance of culturable and citric acid-induced VBNC *S. aureus* under conditions of heat treatment at 63°C. However, Nowakowska and Oliver (3) reported higher resistance of seawater-induced VBNC *V. vulnificus* to heat (50°C), acid (pH 3), and NaCl (5 M) than was seen with their culturable counterparts. Those authors attributed the resuscitation of VBNC *V. vulnificus* strains induced by these stressors to their high stress tolerance (3). In our case, no resuscitation was observed for NTP-induced VBNC *S. aureus* under conditions of exposure to heat, acid, and osmosis (verified by plate count method; data not shown). Differences in the induction conditions and the bacterial strains used resulting in distinct capacities for resuscitation might be the major cause of the contrasting results. Regarding oxidation, higher H_2O_2 resistance of VBNC *S. aureus* than of culturable *S. aureus* was observed in this study. Similarly, enhanced H_2O_2 tolerance in starvation-induced VBNC *V. vulnificus* was also observed previously (3). The antioxidative response induced during VBNC formation might contribute to the development of oxidative resistance in VBNC bacteria. In our study, upregulation was found for the antioxidative response genes (*dps*, *trxA*, *katA*) in VBNC *S. aureus* compared with culturable counterparts. The gene *dps* encodes the protein Dps, which was previously shown to inhibit the occurrence of the H_2O_2-induced Fenton reaction

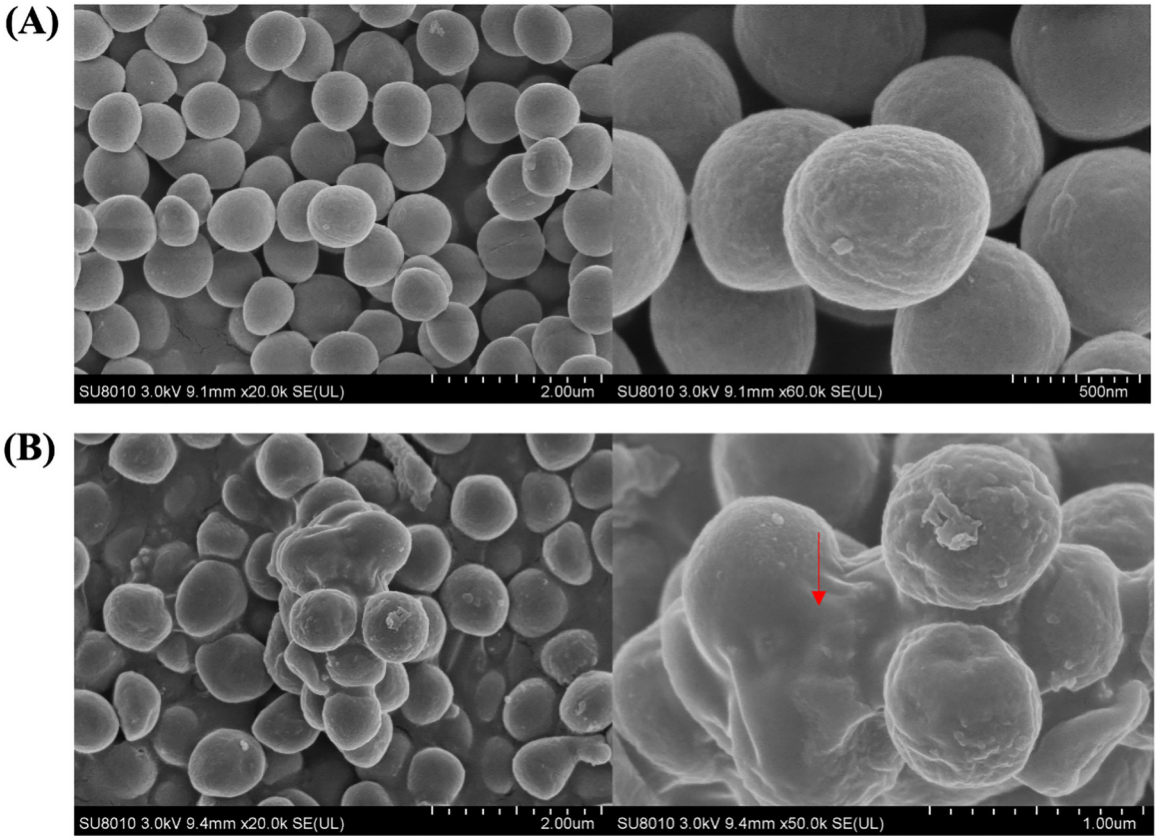

FIG 10 Scanning electron microscopy images of culturable (A) and NTP-induced VBNC (B) *S. aureus*.

to produce the hydroxy radicals (18). Thioredoxins encoded by *trxA* mainly contribute to the maintenance of protein thiols to ensure the reduced state of bacterial cytoplasm upon exposure to oxidative stress (19). The gene *katA* codes for catalase, an important contributor to the detoxification of H_2O_2 into H_2O and O_2 (20). Upregulation of these genes might render VBNC *S. aureus* with resistance to oxidative stress. Similarly, Chen et al. (21) also found that the *soxR* and *katG* antioxidant defense genes were overexpressed in chlorination-induced VBNC *E. coli*.

Higher antibiotic resistance was observed toward ciprofloxacin, chloramphenicol, trimethoprim, and oxacillin in VBNC *S. aureus* compared with culturable strains. Similar results have been reported in previous studies. Lin et al. (22) reported that chlorine-induced VBNC *E. coli* showed higher resistance to a wide range of antibiotics (e.g., ampicillin, gentamicin, and polymyxin). The reasons for the increased capacity of VBNC bacteria against antibiotics are still not clear. One explanation is that overexpression of drug efflux pumps in VBNC bacteria decreases the accumulation of intracellular antibiotic and enhances the related resistance (22). In our study, the *lmrS* multidrug efflux pump gene was found to be significantly expressed in VBNC *S. aureus* compared with culturable *S. aureus*. LmrS encoded by *lmrS* belongs to the major facilitator superfamily (MFS) proteins, which are involved in the efflux of multiple antibiotics, including trimethoprim, chloramphenicol, and linezolid (23). Furthermore, drug tolerance has also been associated with low cellular energy (24). Low metabolic activity is one of the major traits of VBNC bacteria, reflecting the limited cellular energy level (17). In this study, more than half of the metabolic enzymes (e.g., arylamidase, galactosidase, and glucosidase) were confirmed to be suppressed in VBNC *S. aureus*, indicating remarkable metabolism suppression. In order to further estimate the association between cellular energy depletion and antibiotic resistance, CCCP treatment was employed to manually decrease the ATP level in *S. aureus* to achieve a level similar to that of VBNC *S. aureus*.

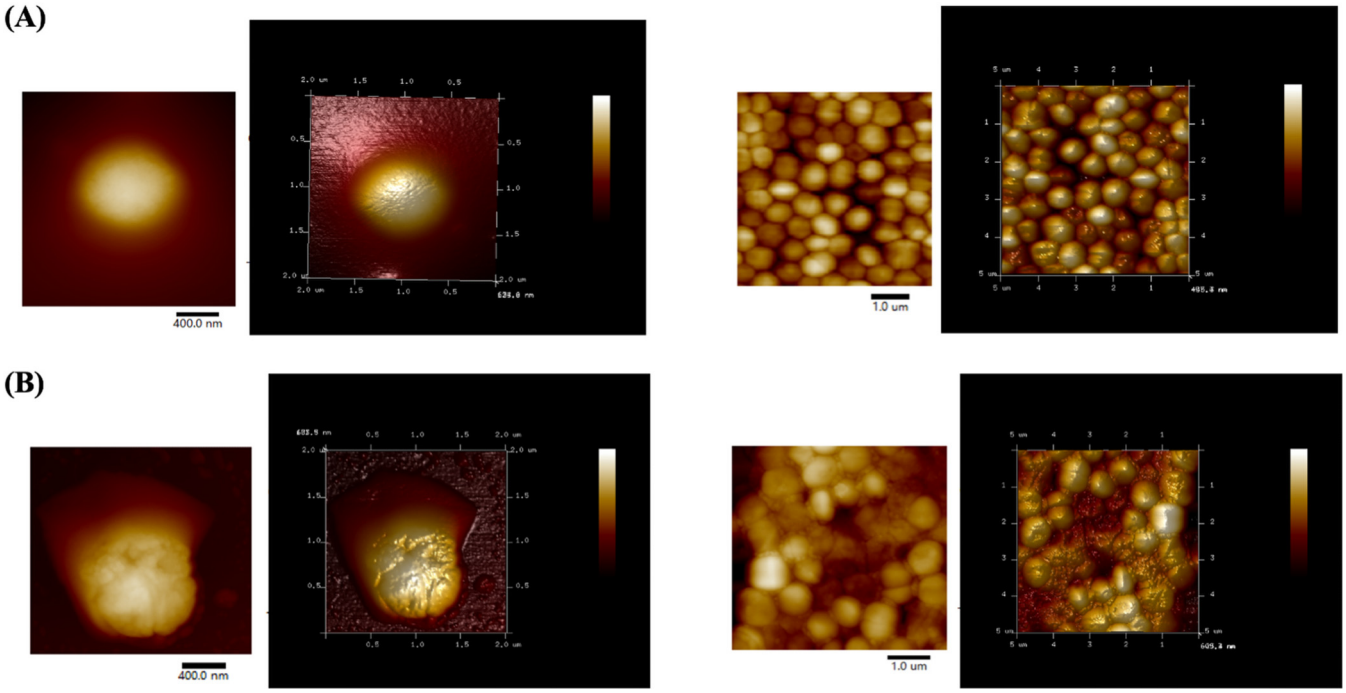

FIG 11 Atomic force microscopy images of culturable (A) and NTP-induced VBNC (B) *S. aureus*.

The tolerance of *S. aureus* to the antibiotics under conditions of ATP depletion was significantly enhanced compared with the tolerance of culturable *S. aureus* with a high ATP level. The low cellular energy is attributed to the decreased activity of energy-dependent antibiotic-targeting pathways, such as DNA replication, protein production, folate biosynthesis, peptidoglycan biosynthesis, and so on, subsequently reducing the efficiency of binding between antibiotics and their targets (25). Additionally, some studies demonstrated that the formation of reactive oxygen species (ROS) might be an additional and common mechanism for the bactericidal action of most antibiotics (26). Therefore, the upregulation in antioxidative responses (*dps*, *trxA*, *katA*) of VBNC *S. aureus* cells might also contribute to the enhanced antibiotic resistance.

In this study, infectious capacity with respect to host cells was found to be retained in VBNC *S. aureus*. Similarly, the pathogenesis of VBNC bacteria was confirmed in previous studies (27, 28). In our work, infection by both VBNC and culturable *S. aureus* caused the induction of the immune response (*TLR2*, *NOD1*) of HeLa cells; however, the expression level of *TLR2* and *NOD1* after infection with VBNC *S. aureus* was found to be lower. The *TLR2* and *NOD1* genes code for the Toll-like receptor (TLR) and nucleotide-binding oligomerization domain (NOD)-like receptor (NLR), respectively, which are the major pattern recognition receptors (PRR) of host cells. These PRRs are responsible for sensing the surface molecules (e.g., peptidoglycan, lipoteichoic acid, lipoproteins) of the invasive pathogens and induce further immune responses, such as apoptosis and secretion of inflammatory factors (e.g., cytokines) (29). The proteomic analysis revealed that the proteins related to lipoteichoic acid and peptidoglycan biosynthesis (LtaS and PBP) were significantly downregulated in VBNC *S. aureus*. LtaS, the lipoteichoic acid synthase, takes part in the production of lipoteichoic acid through catalyzing the polymerization of lipoteichoic acid polyglycerol phosphate from phosphatidylglycerol (PG) (30). Penicillin-binding protein (PBP) mainly contributes to the transglycosylation and transpeptidation steps in the peptidoglycan biosynthesis pathway for glycan strand polymerization and cross-linking between glycan chains, respectively (31). In addition, expression of lipoproteins (QCY65409.1, QCY65537.1, QCY65560.1, QCY67403.1, QCY65601.1, and QCY66887.1) was also found to be suppressed in VBNC *S. aureus*. The reduced expression of these ligands on the bacterial

surface might shield VBNC *S. aureus* from recognition by the host cells and therefore result in reduced levels of immune response induction. Successful adherence to host cells is a prerequisite for the bacterial infections (32). The proteomic analysis in this study revealed that VBNC *S. aureus* depended on two MSCRAMs (microbial surface component recognizing adhesive matrix molecules), ClfB and SdrD, to achieve adherence. Clumping factor B-ClfB is involved in the adherence of *S. aureus* to alpha-chains and beta-chains of immobilized fibrinogen or cytokeratin K10 (K10) of host cells (33). Serine-aspartate repeat-containing protein d (SdrD) mediates the interaction between *S. aureus* and host cells via direct binding to the extracellular matrix of host cells (e.g., desmoglein 1) (34). Additionally, two immune-invasion-associated proteins (SCIN and SasH) were found to be upregulated in VBNC *S. aureus*. Staphylococcal complement inhibitor SCIN contributes to the challenge to the host defense through binding and stabilizing human C3 convertases, which can cause the C3b deposition on the bacterial surface and further phagocytosis (35). The cell wall-anchored protein SasH is involved in the conversion of AMP into adenosine, which further impairs the production of bactericidal factors (e.g., superoxide, nitric oxide) by host cells (36). These changes in the surface virulence factors might be reflected in the overexpression of the protein translocation system (SecG, YajC, and SecE) in VBNC *S. aureus*. In addition to direct invasive actions, VBNC *S. aureus* was also found to enhance the production of extracellular polysaccharide through the upregulation of Cap5B, a capsular biosynthesis protein. The capsule was able to avoid direct assess of the host lysosome to *S. aureus* and enhance its virulence (37). With direct observation by the use of a scanning electron microscope (SEM) and AFM, the extracellular polymeric layer was found to wrap VBNC *S. aureus*, which might also prevent direct attack of the host immune factors (38). As for other virulence factors, the secreted proteins (toxins and exoenzymes) and type VII secretory systems were significantly suppressed in *S. aureus* in its VBNC status, which might be attributable to the limited level of cellular energy (39). The decrease in the levels of most virulence factors contributed to the presence of less damage on host cells, which was confirmed by confocal laser scanning microscopy (CLSM) images indicating that HeLa cells infected with VBNC *S. aureus* retained normal shape with intact nucleus.

During DBD-NTP treatment of *S. aureus*, through multiple electron collision processes (e.g., ionization, dissociative ionization, electron attachment, dissociative electron attachment, excitation, dissociation) and other chemical reactions, the abundant species were produced from plasma discharge. The optical emission spectra indicated that the major plasma species included excited nitrogen (N_2*), charged nitrogen and oxygen (e.g., N_2^+ and O_2^+), and some radicals (e.g., OH, O) (Fig. 1B). When these species arrived at the gas-liquid interface, some of those with a high Henry's constant, such as H_2O_2, OH, HNO_2, and NO_3, were rapidly transported into the liquid phase whereas those with a low Henry's constant, such as O_3, had a limited capacity to enter into the liquid phase. Those transported reactive species in the aqueous phase were further reacted into long-lived species (e.g., H_2O_2, HNO_2/NO_2-, NO_3-, ONOOH/ONOO$-$) in the aqueous medium as the following reactions, which act directly on the bacterial cells. The neutral species (e.g., H_2O_2) could easily get through the cell membrane and subsequently react with the intracellular components. As for the charged species, they might pose a risk of oxidative damage to the external structure of *S. aureus* cells, such as the staphyloxanthin, cell wall, and membranes. Under such a stringent condition, *S. aureus* cells initiated the antioxidant defense system to produce antioxidative proteins (e.g., catalase) to neutralize oxidative species and repair the oxidation-induced damage at the cost of massive energy expenditures. Consequently, the bacterial cells are forced to change their energy allocation and suppress other energy-dependent physiological activities (e.g., cell wall biosynthesis, metabolism) to achieve a "low-energy-consumption" survival pattern-VBNC state (17). Next, we wondered whether the pathogenic bacteria in such a status still retain their risks in food safety and human health.

Therefore, in this study, we continued to evaluate the potential risks of NTP-induced VBNC *S. aureus* compared with culturable *S. aureus*. The levels of thermal, acidic, and osmotic tolerance of VBNC *S. aureus* did not change significantly, while the levels of oxidative and antibiotic resistance were observed to be enhanced. The enhanced

antibiotic resistance could be explained by the decreased cellular energy, the overexpression of multidrug efflux pumps, and the induction of oxidative defense response after entry into VBNC status. In addition, VBNC *S. aureus* retained the ability to infect the HeLa cells through the upregulation of some virulence factors for successful adhesion and internalization. The reduced immune response induced by lower expression of PRRs might prevent recognition of VBNC *S. aureus* by the host cells and enhance the virulence. The camouflaged mechanisms described above enable VBNC *S. aureus* to easily escape from the immune defense of host cells and achieve longer persistence, which poses a potential risk to human health and food safety. Still, more investigation is required to further confirm the general mechanisms for the resistance and pathogenicity development of other strains in a VBNC state.

MATERIALS AND METHODS

Bacterial strains. The *S. aureus* strain (GenBank accession no. CP040801.1) was transferred in tryptic soy broth (TSB) (Base Biotech Co., Hangzhou, China) (17), followed by incubation at 37°C and 180 rpm until the exponential phase. The final concentration of *S. aureus* was found by the plate count method to be around 8 $\log_{10}$ CFU/ml.

Induction of VBNC *S. aureus* with NTP. The NTP generation system (Nanjing Suman Electronics Co., Ltd., Nanjing, China) used in this study was described in detail in our previous study (17). The NTP with an applied energy of 8.1 kJ was applied to treat the *S. aureus* suspension, followed by storage at 4°C for induction of the VBNC state. The final concentration of VBNC *S. aureus* induced under this condition was approximately 7.56 $\log_{10}$ CFU/ml as determined by propidium monoazide quantitative PCR (PMA-qPCR) and plate count methods (17).

Diagnostics of plasma. Optical emission spectroscopy (OES) of the plasma was performed by the use of a Maya200 fiber optic spectrometer (Ocean Optics, Inc., Winter Park, FL, USA) with a spectral resolution of 0.2 nm (40). The fiber probe was placed near the discharge region between two electrodes to detect the optical spectra in the wavelength range of 200 to 800 nm. The collected spectral data were further analyzed with SpectraSuite software (Ocean Optics, Inc.). The active plasma species were identified from the spectra according to previous work (40, 41).

Estimation of viable *S. aureus* levels with PMA-qPCR. The PMA-qPCR method was employed for the enumeration of the total viable *S. aureus* population based on the previous study (17). PMA is a cell membrane-impermeant DNA dye (42). PMA-induced modifications hamper DNA amplification in dead cells; thus, live cells were selectively detected and enumerated with the following qPCR procedure. The *S. aureus* cells were mixed with PMA^{xx} to achieve a final concentration of 50 μM for a 10-min incubation in the dark. Subsequently, a 15-min photolysis procedure was conducted followed by centrifugation (2,320 $\times$ *g* for 10 min) to remove the excess dye. The total DNA was extracted with a TIANamp bacterial DNA kit (Tiangen Biotech Beijing Co., Ltd., Beijing, China) for qPCR detection as follows. Each qPCR system consisted of 2$\times$ master mix (10 μl), RNase/DNase-free water (6.75 μl), carboxy-X-rhodamine (ROX) solution (0.25 μl), the forward and reverse primers of the *nuc* gene (10 μM, 1 μl for each primer), and the template DNA (1 μl), and the qPCR procedure consisted of 1 cycle of 95°C for 2 min; 40 cycles of 95°C for 5 s, 50.2°C for 15 s, and 72°C for 60 s; and 1 cycle of melting curve analysis.

Metabolic enzyme activity in *S. aureus*. The enzymatic activities were determined by the use of an API ZYM kit (bioMérieux SA, Marcy l'Etoile, France) based on the manufacturer's instructions (43). Briefly, the turbidity of *S. aureus* suspensions was adjusted to McFarland standard values of 5 and 6. The bacterial suspension (65 μl) was transferred into each reaction system, followed by incubation at 37°C for 4 h in the dark. Then, one drop of ZYM A and ZYM B reagent was added to each reaction mixture for color development, which was used for the estimation of each enzymatic activity.

Challenge of food-associated stress. Culturable and VBNC *S. aureus* strains were exposed to heat (63°C), oxidation (100 mM H_2O_2), hydrochloric acid (pH 3.0), and osmosis (20% NaCl) challenges. After challenge with stresses, the survival levels of *S. aureus* cells were determined by PMA-qPCR.

Challenge of antibiotics. MICs of oxacillin, ciprofloxacin, chloramphenicol, and trimethoprim (Solarbio Ltd., Beijing, China) were evaluated with a 2-fold broth microdilution method according to Clinical and Laboratory Standards Institute (CLSI) guidelines (44). Briefly, *S. aureus* culture was diluted with Mueller-Hinton broth (MHB; Oxoid, Basingstoke, United Kingdom) to around 6 $\log_{10}$ CFU/ml. Concentrations ranging from 0.125 to 256 μg/ml for each antibiotic were prepared in a 96-well microplate. *S. aureus* culture (100 μl) was mixed with antibiotic solution (100 μl), followed by incubation at 37°C for 24 h. MIC values were then determined by the use of a microplate reader. For challenge with antibiotics, culturable and VBNC *S. aureus* strains were exposed to antibiotics at 10$\times$ MIC at 37°C. After antibiotic challenge, the survival rates of the *S. aureus* cells were determined with PMA-qPCR.

Estimation of gene expression in *S. aureus*. Total RNA of *S. aureus* was extracted with a total RNA purification kit (TR01; GMbiolab Co, Ltd., Taiwan, Republic of China) according to the manufacturer's instructions. The purity and integrity of RNA were estimated with NanoDrop software and electrophoresis. The RNA was subsequently subjected to reverse transcription (RT) into cDNA with a TRUEscript RT kit. Each qPCR volume (20 μl) was established with 10 μl 2$\times$ SYBR green, 2 μl primer mix (Table 2), 1 μl cDNA, and 7 μl RNase/DNase-free water. The qPCR procedure consisted of 52°C for 2 min and 95°C for 2 min for 1 cycle; 95°C for 15 s, 60°C for 30 s, and 72°C for 30 s for 40 cycles; and 65 to 99°C for 1 cycle of melting curve analysis.

TABLE 2 Primers used for gene expression in *S. aureus* cells

Gene	Primer category	Primer sequence (5′–3′)
16S rRNA	F	GTGGAGGGTCATTGGAAACT
	R	CACTGGTGTTCCTCCATATCTC
mepA	F	AGCCACATGATTTCTGCTATCT
	R	CTGCACCAACGCCAAATAAA
norB	F	GTTTCGGACTAGGCTTAGGTATTT
	R	CTGAAGCAACGCCAACTTTATC
lmrS	F	AGGCTGCAACAATAGAACCTAA
	R	CATGATACCTCTGACGGCATATC
kat	F	CAACTGATGGATACGGCTATGA
	R	TTCTTTAGCGTCCTCTGATTGT
dps	F	TACATCATCGCCAGCATTACC
	R	CTGCAGAACAAATGGTTGAAGAA
trxA	F	ACATGGTGTGGTCCATGTAAA
	R	TGTCAGCTTTACCTTCATAGTCAG

ATP depletion in *S. aureus*. Carbonyl cyanide *m*-chlorophenyl hydrazone (CCCP) was added to TSB to achieve a concentration of 10 μM (17). The incubation that followed was conducted at 37°C for 4 h.

Infection of HeLa cells with *S. aureus*. HeLa cells (ATCC CCL-2) were maintained in Eagle's minimum essential medium (MEM) (Thermo Fisher Scientific Inc., Waltham, MA, USA) supplemented with 10% fetal bovine serum (FBS) (Thermo Fisher Scientific) and penicillin-streptomycin liquid (Solarbio Ltd., Beijing, China) (100 U/ml). HeLa cells were seeded on glass coverslips in 24-well plates and cultured for 2 to 3 days until 80% confluence was observed by a light microscope. The infection experiments were conducted in the following procedure (45). Culturable and VBNC *S. aureus* strains were cocultured with HeLa cells at 100 MOI (multiplicity of infection, i.e., the ratio of bacteria per host cell) for 4 h of incubation. Infected cells were washed three times with phosphate-buffered saline (PBS) and then stained with Red CellMask plasma membrane stain (Thermo Fisher Scientific) for 10 min at 37°C. After the staining step, the extract stain was removed and the coverslips were washed with PBS three times, followed by fixation with 4% Formalin (Sigma-Aldrich Corp., St. Louis, MO, USA) for 10 min. After fixation and washing, the cells were permeabilized with 0.1% Triton X-100 for 10 min before staining with DAPI (4′,6-diamidino-2-phenylindole). The adhesion and invasion of bacteria to HeLa cells were observed with a Leica SP8 laser scanning confocal microscope (Leica Microsystems Inc., Buffalo Grove, IL, USA). The images of each sample were obtained with LAS_X_Small_3.0.2 microscopy software (Leica Microsystems Inc.) through the use of the z-stack mode of 28 slices for a thickness of 8 μm. Images were then analyzed using ImageJ software.

Expression of immune response-related genes in infected HeLa cells. Total RNA in uninfected and infected HeLa cells was extracted with RNAiso Plus (TaKaRa Biomedical Technology Co., Ltd., Beijing, China). The purity and concentration of RNA were determined by 1% agarose electrophoresis and the use of a NanoDrop One spectrophotometer. RNA was then reverse transcribed to complementary DNA (cDNA) by the use of a PrimeScript RT reagent kit with genomic DNA (gDNA) Eraser (TaKaRa Biomedical Technology Co., Ltd., Beijing, China). Each qPCR volume (20 μl) included 10 μl of 2× PowerUp SYBR green master mix (Thermo Fisher Scientific), 1 μl of forward and reverse primers (10 μM), 1 μl of cDNA sample, and 7 μl of RNase-free double-distilled water (ddH_2O). The qPCR analysis was performed in a real-time PCR system (QuantStudio 3) with a qPCR run consisting 1 cycle of 2 min at 50°C and 2 min at 95°C followed by 40 cycles of 95°C for 15 s, 60°C for 15 s, and 72°C for 15 s followed by a melting curve. All the primers used are listed in Table 3. The relative expression levels were calculated using the $2^{-\Delta\Delta CT}$ method.

TABLE 3 The primers used for the gene expression of HeLa cells in this study

Gene	Primer category	Primer sequence (5′–3′)	Reference
TLR2	F	GTACCTGTGGGGCTCATTGT	49
	R	CTGCCCTTGCAGATACCATT	
NOD1	F	TCCAAAGCCAAACAGAAACTC	
	R	CAGCATCCAGATGAACGTG	
ACT	F	AAGGTGACAGCAGTCGGTT	50
	R	TGTGTGGACTTGGGAGAGG	

Proteomic analysis of *S. aureus*. After extraction, the protein concentrations were quantified by the use of a bicinchoninic acid (BCA) assay. The extracted proteins were further treated with dithiothreitol (DTT; 1 M) and iodoacetamide (55 mM). Proteins were then subjected to digestion with sequencing-grade modified trypsin (Promega Co., Ltd., Madison, WI, USA). The digested peptide mixture was further labeled with iTRAQ/TMT tags (iTRAQ Reagents 8 Plex [SCIEX]) and were then fractionated using high-pH separation and an Ultimate 3000 system (Thermo Fisher Scientific) connected to a reverse-phase column (XBridge C_{18} column; Waters Corporation, Milford, MA, USA) (4.6 mm by 250 mm, 5-μm pore size). Peptide fractions were then analyzed with an Easy-nLC 1000 system connected to a mass spectrometer (Thermo Fisher Scientific). The mass spectrometry data were then analyzed using the Mascot search engine (Matrix Science, London, United Kingdom). Protein identifications were accepted if they could achieve a false-discovery-rate (FDR) value of less than 1.0% by the Scaffold Local FDR algorithm. The DEPs were defined with a fold change value of >1.2 or <0.83 and an unadjusted significance P value of <0.05. A parallel reaction monitoring (PRM) technique was employed for the verification of the results of the iTrap/TMT proteomic analysis (46). In this study, 11 proteins were randomly selected. After lysis, the proteins were further incubated with Tris(2-carboxyethyl)phosphine (TCEP) (0.5 M) and iodoacetamide (1 M). The digested peptide mixture was desalted by the use of a C_{18} ZipTip, quantified by a Pierce quantitative colorimetric peptide assay, and then lyophilized by the use of a SpeedVac. The library was used for selection of proteotypic peptides and development of PRM assays with the use of SpectroDive software. The sample was then analyzed in unscheduled targeted PRM mode. The peptides were redissolved in solvent A (0.1% formic acid–water) and analyzed using online nanospray liquid chromatography-tandem mass spectrometry (LC-MS/MS) and a Q Exactive high-fidelity (HF) mass spectrometer coupled to an EASY-nLC 1000 system (Thermo Fisher Scientific). Raw files of the targeting runs were analyzed in SpectroDive 9.10 with the default settings. SpectroDive determines the ideal extraction window dynamically. The q value (FDR) cutoff that was applied for the precursor was 1%. Averaged data representing filtered peptides were used to calculate the protein quantities.

Coagulase activity. A solution consisting of VBNC or culturable *S. aureus* (0.8 ml) was added to rabbit blood powder (Kinghunt Ltd., Shanghai, China), followed by incubation at 37°C. The mixture was checked for clotting each hour.

SEM and AFM analysis of *S. aureus*. The treated and control samples were centrifuged at 2,320 $\times$ g and 4°C for 10 min to collect bacterial pellets followed by washing with 0.85% sterile saline solution. The collected bacterial samples were then fixed with 2.5% glutaraldehyde overnight. The following treatment of the fixed bacterial samples was conducted according to the study of Li et al. (47). The samples were finally observed with the use of a SEM (Hitachi model SU8010) (JEOL Co., Ltd., Tokyo, Japan). For AFM analysis, the bacterial samples were placed on the surface of a microscope plate and then dried in air overnight (48). Before analysis, the microscope plate was fixed to an AFM specimen disc with a diameter of 15 mm. The samples were scanned at rate of 1 Hz with a MultiMode AFM (Veeco Instruments Inc., Oyster Bay, NY, USA) operated in the tapping mode. The obtained AFM images were further processed with NanoScope Analysis software.

Data availability. Strain S15 whole-genome data have been submitted to GenBank (accession number CP040801).

ACKNOWLEDGMENTS

This study was supported by the National Natural Science Foundation of China (grant 31772079).

We have no conflict of interest to declare.

REFERENCES

1. Zhao X, Zhong J, Wei C, Lin C, Ding T. 2017. Current perspectives on viable but non-culturable state in foodborne pathogens. Front Microbiol 8:580. https://doi.org/10.3389/fmicb.2017.00580.
2. Dong K, Pan H, Yang D, Rao L, Zhao L, Wang Y, Liao X. 2020. Induction, detection, formation, and resuscitation of viable but non-culturable state microorganisms. Compr Rev Food Sci Food Saf 19:149–183. https://doi.org/10.1111/1541-4337.12513.
3. Nowakowska J, Oliver JD. 2013. Resistance to environmental stresses by Vibrio vulnificus in the viable but nonculturable state. FEMS Microbiol Ecol 84:213–222. https://doi.org/10.1111/1574-6941.12052.
4. Yaron S, Matthews K. 2002. A reverse transcriptase-polymerase chain reaction assay for detection of viable *Escherichia coli* O157:H7: investigation of specific target genes. J Appl Microbiol 92:633–640. https://doi.org/10.1046/j.1365-2672.2002.01563.x.
5. Highmore C, Warner J, Rothwell S, Wilks S, Keevil C. 2018. Viable-but-nonculturable *Listeria monocytogenes* and *Salmonella enterica* serovar Thompson induced by chlorine stress remain infectious. mBio 9:e00540-18. https://doi.org/10.1128/mBio.00540-18.
6. Zhao F, Wang Y, An H, Hao Y, Hu X, Liao X. 2016. New insights into the formation of viable but nonculturable *Escherichia coli* O157:H7 induced by high-pressure CO_2. mBio 7:e00961-16. https://doi.org/10.1128/mBio.00961-16.
7. Liao H, Zhang R, Zhong K, Ma Y, Nie X, Liu Y. 2018. Induction of a viable but non-culturable state in *Salmonella* Typhimurium is correlated with free radicals generated by thermosonication. Int J Food Microbiol 286:90–97. https://doi.org/10.1016/j.ijfoodmicro.2018.07.017.
8. Bai H, Zhao F, Li M, Qin L, Yu H, Lu L, Zhang T. 2019. Citric acid can force *Staphylococcus aureus* into viable but nonculturable state and its characteristics. Int J Food Microbiol 305:108254. https://doi.org/10.1016/j.ijfoodmicro.2019.108254.
9. Muhammad AI, Liao X, Cullen PJ, Liu D, Xiang Q, Wang J, Chen S, Ye X, Ding T. 2018. Effects of nonthermal plasma technology on functional food components. Comp Rev Food Sci Food Saf 17:1379–1394. https://doi.org/10.1111/1541-4337.12379.
10. Liao X, Muhammad AI, Chen S, Hu Y, Ye X, Liu D, Ding T. 2019. Bacterial spore inactivation induced by cold plasma. Crit Rev Food Sci Nutr 59:2562–2572. https://doi.org/10.1080/10408398.2018.1460797.
11. Liao X, Li J, Muhammad AI, Suo Y, Chen S, Ye X, Liu D, Ding T. 2018. Application of a dielectric barrier discharge atmospheric cold plasma (Dbd-Acp) for *Escherichia coli* inactivation in apple juice: inactivation of *E. coli* by cold plasma. J Food Sci 83:401–408. https://doi.org/10.1111/1750-3841.14045.
12. Muhammad AI, Lv R, Liao X, Chen W, Liu D, Ye X, Chen S, Ding T. 2019. Modeling the inactivation of *Bacillus cereus* in tiger nut milk treated with

cold atmospheric pressure plasma. J Food Prot 82:1828–1836. https://doi.org/10.4315/0362-028X.JFP-18-586.
13. Bourke P, Ziuzina D, Boehm D, Cullen PJ, Keener K. 2018. The potential of cold plasma for safe and sustainable food production. Trends Biotechnol 36:615–626. https://doi.org/10.1016/j.tibtech.2017.11.001.
14. Liao X, Liu D, Xiang Q, Ahn J, Chen S, Ye X, Ding T. 2017. Inactivation mechanisms of non-thermal plasma on microbes: a review. Food Control 75:83–91. https://doi.org/10.1016/j.foodcont.2016.12.021.
15. Joaquin J, Kwan C, Abramzon N, Vandervoort K, Brelles-Marino G. 2009. Is gas-discharge plasma a new solution to the old problem of biofilm inactivation? Microbiology (Reading) 155:724–732. https://doi.org/10.1099/mic.0.021501-0.
16. Cooper M, Fridman G, Fridman A, Joshi S. 2010. Biological responses of *Bacillus stratosphericus* to floating electrode-dielectric barrier discharge plasma treatment. J Appl Microbiol 109:2039–2048. https://doi.org/10.1111/j.1365-2672.2010.04834.x.
17. Liao X, Liu D, Ding T. 2020. Nonthermal plasma induces the viable-but-nonculturable state in *Staphylococcus aureus* via metabolic suppression and the oxidative stress response. Appl Environ Microbiol 86:e02216-19. https://doi.org/10.1128/AEM.02216-19.
18. Ushijima Y, Yoshida O, Villanueva M, Ohniwa R, Morikawa K. 2016. Nucleoid clumping is dispensable for the Dps-dependent hydrogen peroxide resistance in *Staphylococcus aureus*. Microbiology (Reading) 162:1822–1828. https://doi.org/10.1099/mic.0.000353.
19. Uziel O, Borovok I, Schreiber R, Cohen G, Aharonowitz Y. 2004. Transcriptional regulation of the *Staphylococcus aureus* thioredoxin and thioredoxin reductase genes in response to oxygen and disulfide stress. J Bacteriol 186:326–334. https://doi.org/10.1128/jb.186.2.326-334.2004.
20. Chelikani P, Fita I, Loewen P. 2004. Diversity of structures and properties among catalases. Cell Mol Life Sci 61:192–208. https://doi.org/10.1007/s00018-003-3206-5.
21. Chen S, Li X, Wang Y, Zheng J, Ye C, Li X, Guo L, Zhang S, Yu X. 2018. Induction of *Escherichia coli* into a VBNC state through chlorination/chloramination and differences in characteristics of the bacterium between states. Water Res 142:279–288. https://doi.org/10.1016/j.watres.2018.05.055.
22. Lin H, Ye C, Chen S, Zhang S, Yu X. 2017. Viable but non-culturable *E. coli* induced by low level chlorination have higher persistence to antibiotics than their culturable counterparts. Environ Pollut 230:242–249. https://doi.org/10.1016/j.envpol.2017.06.047.
23. Floyd J, Smith K, Kumar S, Floyd J, Varela M. 2010. LmrS is a multidrug efflux pump of the major facilitator superfamily from *Staphylococcus aureus*. Antimicrob Agents Chemother 54:5406–5412. https://doi.org/10.1128/AAC.00580-10.
24. Robben C, Witte AK, Schoder D, Stessl B, Rossmanith P, Mester P. 2019. A fast and easy ATP-based approach enables MIC testing for non-resuscitating VBNC pathogens. Front Microbiol 10:1365. https://doi.org/10.3389/fmicb.2019.01365.
25. Conlon B, Rowe S, Gandt A, Nuxoll A, Donegan N, Zalis E, Clair G, Adkins J, Cheung A, Lewis K. 2016. Persister formation in *Staphylococcus aureus* is associated with ATP depletion. Nat Microbiol 1:16051. https://doi.org/10.1038/nmicrobiol.2016.51.
26. Kohanski M, Dwyer D, Hayete B, Lawrence C, Collins J. 2007. A common mechanism of cellular death induced by bactericidal antibiotics. Cell 130:797–810. https://doi.org/10.1016/j.cell.2007.06.049.
27. Wong H, Shen C, Chang C, Lee Y, Oliver JD. 2004. Biochemical and virulence characterization of viable but nonculturable cells of *Vibrio parahaemolyticus*. J Food Prot 67:2430–2435. https://doi.org/10.4315/0362-028x-67.11.2430.
28. Baffone W, Citterio B, Vittoria E, Casaroli A, Campana R, Falzano L, Donelli G. 2003. Retention of virulence in viable but non-culturable halophilic Vibrio spp. Int J Food Microbiol 89:31–39. https://doi.org/10.1016/S0168-1605(03)00102-8.
29. Chamaillard M, Hashimoto M, Horie Y, Masumoto J, Qiu S, Saab L, Ogura Y, Kawasaki A, Fukase K, Kusumoto S, Valvano MA, Foster SJ, Mak TW, Nuñez G, Inohara N. 2003. An essential role for NOD1 in host recognition of bacterial peptidoglycan containing diaminopimelic acid. Nat Immunol 4:702–707. https://doi.org/10.1038/ni945.
30. Schneewind O, Missiakas D. 2014. Lipoteichoic acids, phosphate-containing polymers in the envelope of gram-positive bacteria. J Bacteriol 196:1133–1142. https://doi.org/10.1128/JB.01155-13.
31. Reed P, Atilano ML, Alves R, Hoiczyk E, Sher X, Reichmann NT, Pereira PM, Roemer T, Filipe SR, Pereira-Leal JB, Ligoxygakis P, Pinho MG. 2015. *Staphylococcus aureus* survives with a minimal peptidoglycan synthesis machine but sacrifices virulence and antibiotic resistance. PLoS Pathog 11:e1004891. https://doi.org/10.1371/journal.ppat.1004891.
32. Josse J, Laurent F, Diot A. 2017. Staphylococcal adhesion and host cell invasion: fibronectin-binding and other mechanisms. Front Microbiol 8:2433. https://doi.org/10.3389/fmicb.2017.02433.
33. Walsh E, O'Brien L, Liang X, Hook M, Foster T. 2004. Clumping factor B, a fibrinogen-binding MSCRAMM (microbial surface components recognizing adhesive matrix molecules) adhesin of *Staphylococcus aureus*, also binds to the tail region of type I cytokeratin 10. J Biol Chem 279:50691–50699. https://doi.org/10.1074/jbc.M408713200.
34. Askarian F, Ajayi C, Hanssen A, Van Sorge N, Pettersen I, Diep D, Sollid J, Johannessen M. 2016. The interaction between *Staphylococcus aureus* SdrD and desmoglein 1 is important for adhesion to host cells. Sci Rep 6:22134. https://doi.org/10.1038/srep22134.
35. Rooijakkers S, Ruyken M, Van Roon J, Van Kessel K, Van Strijp J, Van Wamel W. 2006. Early expression of SCIN and CHIPS drives instant immune evasion by *Staphylococcus aureus*. Cell Microbiol 8:1282–1293. https://doi.org/10.1111/j.1462-5822.2006.00709.x.
36. Thammavongsa V, Kern J, Missiakas D, Schneewind O. 2009. Staphylococcus aureus synthesizes adenosine to escape host immune responses. J Exp Med 206:2417–2427. https://doi.org/10.1084/jem.20090097.
37. Kim K, Elliott S, Di Cello F, Stins M, Kim K. 2003. The K1 capsule modulates trafficking of *E. coli*-containing vacuoles and enhances intracellular bacterial survival in human brain microvascular endothelial cells. Cell Microbiol 5:245–252. https://doi.org/10.1046/j.1462-5822.2003.t01-1-00271.x.
38. Bagnoli F, Rappuoli R. 2017. Protein and sugar export and assembly in Gram-positive bacteria. Springer International Publishing, Basel, Switzerland.
39. Tuchscherr L, Heitmann V, Hussain M, Viemann D, Roth J, von Eiff C, Peters G, Becker K, Löffler B. 2010. *Staphylococcus aureus* small-colony variants are adapted phenotypes for intracellular persistence. J Infect Dis 202:1031–1040. https://doi.org/10.1086/656047.
40. Guo J, Li Z, Huang K, Li Y, Wang J. 2017. Morphology analysis of *Escherichia coli* treated with nonthermal plasma. J Appl Microbiol 122:87–96. https://doi.org/10.1111/jam.13335.
41. Sarangapani C, Misra NN, Milosavljevic V, Bourke P, O'Regan F, Cullen PJ. 2016. Pesticide degradation in water using atmospheric air cold plasma. J Water Process Eng 9:225–232. https://doi.org/10.1016/j.jwpe.2016.01.003.
42. Nocker A, Cheung C, Camper A. 2006. Comparison of propidium monoazide with ethidium monoazide for differentiation of live vs. dead bacteria by selective removal of DNA from dead cells. J Microbiol Methods 67:310–320. https://doi.org/10.1016/j.mimet.2006.04.015.
43. Zhao F, Bi X, Hao Y, Liao X. 2013. Induction of viable but nonculturable *Escherichia coli* O157:H7 by high pressure CO_2 and its characteristics. PLoS One 8:e62388. https://doi.org/10.1371/journal.pone.0062388.
44. Ma Y, Lan G, Li C, Cambaza EM, Liu D, Ye X, Chen S, Ding T. 2019. Stress tolerance of *Staphylococcus aureus* with different antibiotic resistance profiles. Microb Pathog 133:103549. https://doi.org/10.1016/j.micpath.2019.103549.
45. Merghni A, Ben Nejma M, Helali I, Hentati H, Bongiovanni A, Lafont F, Aouni M, Mastouri M. 2015. Assessment of adhesion, invasion and cytotoxicity potential of oral *Staphylococcus aureus* strains. Microb Pathog 86:1–9. https://doi.org/10.1016/j.micpath.2015.05.010.
46. Li M, Zhang K, Long R, Sun Y, Kang J, Zhang T, Cao S. 2017. iTRAQ-based comparative proteomic analysis reveals tissue-specific and novel early-stage molecular mechanisms of salt stress response in Carex rigescens. Environ Exp Bot 143:99–114. https://doi.org/10.1016/j.envexpbot.2017.08.010.
47. Li J, Ding T, Liao X, Chen S, Ye X, Liu D. 2017. Synergetic effects of ultrasound and slightly acidic electrolyzed water against *Staphylococcus aureus* evaluated by flow cytometry and electron microscopy. Ultrason Sonochem 38:711–719. https://doi.org/10.1016/j.ultsonch.2016.08.029.
48. Li J, Suo Y, Liao X, Ahn J, Liu D, Chen S, Ye X, Ding T. 2017. Analysis of *Staphylococcus aureus* cell viability, sublethal injury and death induced by synergistic combination of ultrasound and mild heat. Ultrason Sonochem 39:101–110. https://doi.org/10.1016/j.ultsonch.2017.04.019.
49. Al-Sayeqh A, Loughlin M, Dillon E, Mellits K, Connerton I. 2010. *Campylobacter jejuni* activates NF-κB independently of TLR2, TLR4, Nod1 and Nod2 receptors. Microb Pathog 49:294–304. https://doi.org/10.1016/j.micpath.2010.06.011.
50. Jiang N, Xie F, Guo Q, Li M, Xiao J, Sui L. 2017. Toll-like receptor 4 promotes proliferation and apoptosis resistance in human papillomavirus–related cervical cancer cells through the Toll-like receptor 4/nuclear factor-κB pathway. Tumour Biol 2017:1–9. https://doi.org/10.1177/1010428317710586.